Pergamon

Int. J. Solids Structures Vol. 34, No. 18, pp. 2291–2301, 1997

0020–7683/97 $17.00 + .00

PII : S0020–7683(96)00146–1

# VIBRATION AND BUCKLING ANALYSIS OF RECTANGULAR PLATES WITH NONLINEAR ELASTIC END RESTRAINTS AGAINST ROTATION

T.-P. CHANG* and H.-C. CHANG
Department of Applied Mathematics, National Chung-Hsing University, Taichung, Taiwan, Republic of China

(*Received* 11 *October* 1995; *in revised form* 2 *July* 1996)

**Abstract**—The fundamental natural frequencies and buckling loads of a rectangular plate with nonlinearly rotational restraints are obtained by using the finite element technique. If the rotational springs are unsymmetric the iterative scheme must be employed to acquire the solutions of the nonlinear problem. The values which describe the free vibration and stability behaviour of the plate will increase when either the parameters of rotational spring or the initial rotational angles increase. Incidentally, it can be concluded that these results grown nonlinearly with respect to either the linear or nonlinear rotational spring constants. Finally, both the frequency and stability parameters are evaluated for several boundary conditions which are quite useful in engineering analysis and design.


## 1. INTRODUCTION

Investigations on the problem of nonlinear vibration and buckling have been interesting and challenging. In particular, the vibration and buckling of system with nonlinear boundary conditions are studied in this study. Although the available literature regarding this subject is not very large, among others, the following researchers have already contributed to the development of this field. Hartog (1936) performed the forced vibration analysis in nonlinear systems with various combinations of linear springs. The nonlinear vibration of a hinged-hinged bar was studied by Woinowsky-Krieger (1950). Paslay and Gurtin (1960) investigated the vibration response of a linear undamped system resting on a nonlinear spring. Wah (1964) studied the nonlinear vibrations with various boundary conditions in which the solution was presented in terms of normal modes. Porter and Billet (1965) investigated the harmonic and sub-harmonic vibration of a continuous system with nonlinear constraint. Meanwhile, Taucher and Ayre (1965) studied the shock response of a simple beam on nonlinear supports. Dokainish and Kumar (1971) performed the experimental and theoretical analysis of the transverse vibrations of a beam with bilinear support. Bhashyam and Prathap (1980) and Sarma and Varadan (1983) used different types of finite element method, which are Galerkin and Lagrange types, respectively, to analyze the nonlinear behaviour of beams with simply supported and clamped conditions. Prathap (1978) studied the nonlinear vibration of a beam with a variable axial restraint. Laura and Romanelli (1974) used the Galerkin method to investigate the vibration and buckling of rectangular plates elastically restrained against rotation along all edges and subjected to a biaxial state of stress. Warburton and Edney (1984) adopted the Ritz method to perform the vibration and buckling analysis of rectangular plates with elastically restrained edges. Bennouna and White (1984) studied the effect of large vibration amplitude in the fundamental mode shape of a clamped-clamped uniform beam and presented their results on the fundamental resonance frequency as a function of the amplitude to beam thickness ratio. Meanwhile, Chi *et al.* (1984) studied the linear free vibrations of a uniform beam with rotationally restrained ends subjected to axial forces. The importance of rotational boundary conditions was experimentally investigated by Picard *et al.* (1987). Liu *et al.* (1988) investigated the approximate nonlinear free vibration frequencies analytically for uniform beams with both ends restrained by rotational springs with different degrees of restraint. Gutierrez *et al.* (1990) used the finite element method to analyze the fundamental frequency of vibration of a Timoshenko beam with non-uniform thickness. Also, Rao and Naidu (1994) studied the free vibration and stability behaviour of a simply supported uniform beam with nonlinear elastic end restraints against rotation.

In this study, the system considered might be a simple representation of structures where the range of deflections is such that the motion of the plate can be described by a linear partial differential equation but the assumption of linear rotational boundary conditions may not be admissible; in fact, the nonlinear rotational boundary conditions are considered. The purpose of this study is to analyze the free vibration problem, the free vibration with initial in-plane stresses problem and stability behaviour of a rectangular plate with boundaries elastically restrained against rotation. Numerical results are calculated for both symmetric or unsymmetric restraints. Noting that the iterative scheme is needed when the rotational springs at both edges are unsymmetric, otherwise the symmetric problem can be solved without any method for convergence. The solutions to these problems are quite useful in engineering analysis and design.

## 2. FINITE ELEMENT FORMULATION

Consider the case of a rectangular thin plate of dimension $a \times b$, thickness $h$, Poisson's ratio $v$ and Young's modulus $E$ with nonlinear rotational restraints at left edge $AD$ and right edge $BC$, as shown in Fig. 1. Due to the nonlinear property of the boundary condition, the finite element method is adopted to perform the free vibration and stability analysis. In this study, a simple and efficient finite element is used, as shown in Fig. 2, this kind of plate finite element contains four degrees of freedom at each of the four corner nodes: $w$, $w_x$, $w_y$, $w_{xy}$, where $w$ is the transverse displacement of the plate, $w_x = \partial w/\partial x$, $w_y = \partial w/\partial y$, and $w_{xy} = \partial^2 w/\partial x \partial y$. It should be noted that with these element displacement functions it was found that the inclusion of the twist in addition to the displacement and slope at the corner of an element achieved a remarkable improvement in accuracy of the computed natural frequencies and mode shapes. Furthermore, the researchers and specialists think that the fundamental mode always has lowest error when four unknowns at each corner are adopted, that the modes with at least three nodal lines in one direction always have lower error that the modes with four nodal lines and the relative position of any mode remains as the number of elements increase. The rotational spring restraints at both edges are defined as

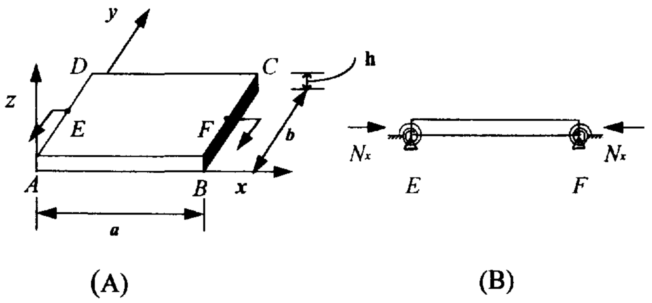


Fig. 1. Configuration of the problem.

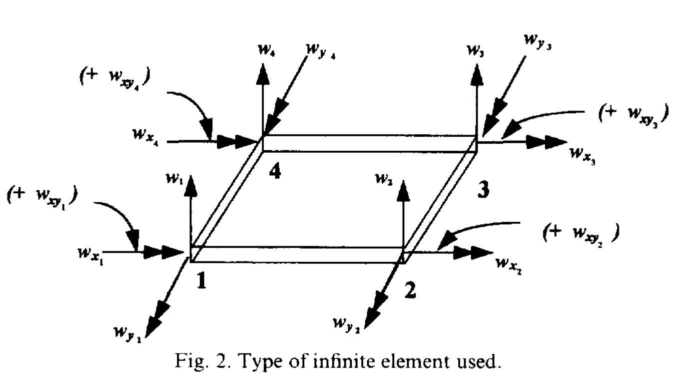


Fig. 2. Type of infinite element used.

$$M_L = \zeta_L w_x(0, y) + \eta_L w_x^3(0, y) \tag{1}$$

and

$$M_R = \zeta_R w_x(a, y) + \eta_R w_x^3(a, y) \tag{2}$$

where $M_L$ and $M_R$ are bending moments at left and right side, respectively, $\zeta_L$, $\zeta_R$, $\eta_L$, $\eta_R$ are the constants which determines the spring behaviour, respectively.

The strain energy expression for a bending plate is known as

$$U_1 = \int\int \frac{D}{2}\left[\left(\frac{\partial^2 w}{\partial x^2}\right)^2 + \left(\frac{\partial^2 w}{\partial y^2}\right)^2 + 2\nu\left(\frac{\partial^2 w}{\partial x^2}\right)\left(\frac{\partial^2 w}{\partial x^2}\right) + 2(1-\nu)\left(\frac{\partial^2 w}{\partial x \partial y}\right)^2\right] dx\, dy \tag{3}$$

where $D = Eh^3/12(1-\nu)$ is the elastic rigidity of the plate.

The kinetic energy for a vibration plate in bending with small deflection is

$$T = \frac{\rho h}{2}\int\int (\dot{w})^2\, dx\, dy \tag{4}$$

where $\rho$ is the mass density per volume of the plate.

In buckling analysis, the work done in a plate element due to the in-plane forces must be considered and which can be obtained as

$$U_2 = \tfrac{1}{2}\int\int [N_x(w_x)^2 + N_y(w_y)^2 + 2N_{xy} w_x w_y]\, dx\, dy \tag{5}$$

where $N_x$, $N_y$, $N_{xy}$ are axial loads in the corresponding directions, respectively.

Express $w$ in terms of the shape functions $N^i$ and nodal displacements $W^i$ as follows

$$w = [N^i][W^i] \tag{6}$$

where the superscripts denote the summation of all nodal displacements of the element. The finite element equation of the problem can be formulated by using the following Lagrange's equation:

$$\frac{d}{dt}\left(\frac{\partial T}{\partial \dot{w}}\right) + \frac{\partial U}{\partial w} = F_i. \tag{7}$$

The first term on the left of eqn (7) produces the mass matrix $[m]$ and if we combine $U_1$ and $U_2$ as the total strain energy $U$, the second term produces the stiffness matrix $[k]$ and incremental stiffness matrix $[g]$, it should be noted that if the forces $N_x$, $N_y$ and $N_{xy}$ are not constants, the problem becomes more involved. For convenience, we assume the relationship for these forces are mutually proportional to one another, i.e. $N_x = -\lambda$, $N_y = -c_1\lambda$ and $N_{xy} = -c_2\lambda$, where $c_1$ and $c_2$ are two positive constants and then combine the stiffness matrix with the mass matrix, the eigenvalue problem will be stated as

$$\{[k] - \lambda[g] - \omega^2[m]\}[W] = 0 \tag{8}$$

where $\omega$ is the natural frequency and $\lambda$ is the stability parameter. However, the effects of nonlinear rotational spring restraints are the goal of this study. The work done in a plate element due to this restraint at left edge is formulated as

$$U_3 = \tfrac{1}{2}\int M_L w_{,x}(0,y)\,dy$$
$$= \tfrac{1}{2}\int\{\zeta_L[w_{,x}(0,y)]^2 + \eta_L[w_{,x}(0,y)]^4\}\,dy$$
$$= \tfrac{1}{2}\int\{\zeta_L([N^i_{,x}][W^i(0,y)])^2 + \eta_L([N^i_{,x}][W^i(0,y)])^4\}\,dy. \tag{9}$$

By using the Castigliano's theorem, the equivalent spring stiffness coefficients of left edge are

$$k^*_{ij} = \frac{\partial^2 U_3}{\partial W^i \partial W^i}$$
$$= \int\{\zeta_L(N^i_{,x}N^i_{,x}) + 6\eta_L([N^i_{,x}][W^i])^2 N^i_{,x}N^i_{,x}\}\,dy. \tag{10}$$

Similarly, we proceed to deal with the nonlinear rotational spring restraints at right edge by the same procedure and then the other equivalent spring stiffness coefficients $[k^{**}_{ij}]$ are obtained. Both matrices $[k^*_{ij}]$ and $[k^{**}_{ij}]$ have to be added into the corresponding positions of the stiffness matrix $[k]$. Consequently, the resulting matrix equation after assembly can be derived as

$$\{[K(W')] - \lambda[G] - \omega^2[M]\}[W] = 0. \tag{11}$$

We can solve eqn (11) by using any standard algorithm to obtain eigenvalues. Noting that the assembled stiffness matrix contains terms consisting of $W'$ because of the nonlinear part of the rotational elastic restraint. However, as previous discussion, these nonlinear terms only appear at some corresponding positions of the stiffness matrix. It is sufficient if one assembles the value of $W'$ and for this value of $W'$ the solution can be directly obtained for a given spring constants of $\zeta_L$, $\zeta_R$, $\eta_L$ and $\eta_R$.

It is known that eqn (11) can be used to solve several types of problem as follows:

(1) When the incremental stiffness matrix $[G]$ is absent, eqn (11) states a free vibration problem. Furthermore, the natural frequencies and mode shapes obtained can be used to treat dynamic response problems of plates using the method of modal analysis.

(2) When the mass matrix $[M]$ is absent, it states a stability problem. The eigenvalues $\lambda$ are the buckling loads and $[W]$ are the buckling mode shapes.

(3) When both the incremental stiffness matrix and mass matrix are present, it states a free vibration problem of plates with initial in-plane stresses.

In order to solve eqn (11), the iteration procedure is needed if the spring constants are unsymmetrical. This scheme is briefly stated as follows:

(i) At beginning, all values of $W'$ in stiffness matrix are artificially set to be zeroes and then solve eqn (11) to obtain the eigenvalues and eigenvectors.

(ii) Adjust the eigenvector values at left edge to the prescribed values, i.e. all eigenvectors are multiplied by a scalar at this stage.

(iii) The values of $W'$ in equivalent spring stiffness matrices are updated by the values which evaluated at stage (ii).

(iv) Add equivalent spring stiffness matrices obtained at stage (iii) into some positions of stiffness matrix.

(v) Resolve the eigenvalue problem of eqn (11) in which the stiffness matrix is updated and then the new eigenvalues are obtained.

(vi) Repeat stages (ii)–(v) until all the eigenvector values at right edge converge to an expected accuracy.

Table 1. Convergence of fundamental natural frequencies vs number of elements

| | Number of elements | | | | | | |
|---|---|---|---|---|---|---|---|
| | 16 | 64 | 144 | 196 | 256 | 324 | Exact |
| (A) | 62.11 | 61.92 | 61.73 | 61.66 | 61.60 | 61.56 | 61.11 |
| (B) | 151.86 | 65.03 | 62.48 | 62.06 | 61.82 | 61.59 | — |
| (C) | 35.06 | 29.12 | 29.04 | 29.03 | 29.02 | 29.02 | — |

(A) is the simply-supported case without restraint.
(B) is the simply-supported case with $\zeta = 100$ (lb-in/in- ), $\eta = 10{,}000$ (lb-in/in-$^{3}$) of case (1).
(C) is the free case with $\zeta = 10$ (lb-in/in- ), $\eta = 100$ (lb-in/in-$^{3}$) of case (1).

## 3. NUMERICAL ANALYSIS AND DISCUSSION

In this study, the following parameter values are used for describing the material and geometry of the rectangular plate: $a = b = 144$ in (3.66 m), $h = 3.0$ in (7.62 cm), $E = 10{,}000$ Ksi ($6.89 \times 10^{10}$ N m$^{-2}$), $\nu = 0.3$, $\rho = 41.47$ slug ft$^{-3}$ ($2.14 \times 10^{4}$ kg m$^{-3}$), where $a$, $b$, $h$, $E$, $\nu$, $\rho$ are dimensions, thickness, Young's modulus of elasticity, Poisson's ratio and mass density, respectively. The total numbers of finite element is 64. The computer programs are coded on HP 835/SRX to perform numerical analysis for the problem.

In the first place, a convergence study about the behaviour of the natural frequency values is presented in Table 1. As it can be seen from part (A) of Table 1, the convergence of the fundamental natural frequency is justified as the number of the elements is increased. Although there are no exact solutions available for parts (B) and (C) of Table 1 which have nonlinear rotational restraints, the convergences of the fundamental natural frequency are still manifested for the free and simply-supported cases as it can be detected from Table 1. As to the check of the accuracy of the buckling load, the comparison of buckling loads for limit cases with the results obtained by other means are presented in Table 2. It should be noted that the results computed by the present study must be transformed into dimensionless expressions in order to be compared with the other results. As it can be found from Table 2, the buckling loads for limit cases show a fairly good agreement.

The variation of fundamental frequencies and critical loads of the rectangular plate are obtained with respect to a few different spring constants at both edges and presented in the form of tables, respectively, the fundamental frequencies influenced by axial forces are shown in the form of figures. In this study, the plate with several kinds of boundary conditions are investigated to illustrate the application of the proposed method, i.e. the boundary conditions at both edges with nonlinear elastic rotational restraints are assumed to be simply-supported and those of the other two edges are assumed as the following three different cases: simply–simply (Tables 3–5), clamped–clamped (Tables 6–8) and free–free (Tables 9–11). The parameters of rotational springs are denoted by $\zeta$ and $\eta$, respectively, as a symmetric configuration, i.e. $\zeta_L = \zeta_R = \zeta$ and $\eta_L = \eta_R = \eta$. The unsymmetric spring constants applied on the plate are presented in Tables 12–14 which the edges without restraints are assumed to be free–free.

In Table 3, the fundamental natural frequencies for simply–simply case are presented. The given angle values of case (2) are twice as those of case (1) three times for case (3), etc. The nodal rotational angles from the left bottom corner to the midpoint of left edge in case (1) are assumed to be 0.01, 0.088, 0.157, 0.204 and 0.221, in degrees, for simply–simply case. Incidentally, they are assumed to be 0.0, 0.01, 0.032, 0.053, 0.062 and 0.01, 0.0094, 0.0091, 0.0089, 0.0088, in degrees, for clamped–clamped and free–free cases, respectively.

Table 2. Comparison of buckling loads for limit cases

| | Timoshenko (1961) | Laura (1974) | Warburton (1984) | Present study |
|---|---|---|---|---|
| Simply-supported case | 19.739 | — | 19.739 | 20.282 |
| Clamped case | 52.310 | 54.000 | 52.990 | 53.432 |

Table 3. Variation of fundamental natural frequencies (rad $s^{-1}$) for simply–simply case

| | | Initial rotational angles on left side (degrees) | | | | |
|---|---|---|---|---|---|---|
| $\zeta$(lb-in/in$^{-2}$) | $\eta$(lb-in/in$^{-3}$) | case (1) | case (2) | case (3) | case (4) | case (5) |
| 0 | 0 | 61.92 | 61.92 | 61.92 | 61.92 | 61.92 |
| 0 | 10 000 | 64.90 | 72.23 | 80.99 | 89.15 | 95.93 |
| 10 | 100 | 61.97 | 62.06 | 62.22 | 62.44 | 62.71 |
| 10 | 10 000 | 64.91 | 72.24 | 80.99 | 89.15 | 95.93 |
| 100 | 100 | 62.11 | 62.20 | 62.35 | 62.57 | 62.84 |
| 100 | 10,000 | 65.03 | 72.33 | 81.06 | 89.19 | 95.96 |

Table 4. Variation of buckling loads (lb $in^{-1}$) under $N_x$ for simply–simply case

| | | Initial rotational angles on left side (degrees) | | | | |
|---|---|---|---|---|---|---|
| $\zeta$(lb-in/in$^{-2}$) | $\eta$(lb-in/in$^{-3}$) | case (1) | case (2) | case (3) | case (4) | case (5) |
| 0 | 0 | 48 303 | 48 303 | 48 303 | 48 303 | 48 303 |
| 0 | 10 000 | 52 966 | 64 354 | 76 126 | 84 073 | 88 632 |
| 10 | 100 | 48 375 | 48 522 | 48 764 | 49 102 | 49 533 |
| 10 | 10 000 | 52 987 | 64 369 | 76 134 | 84 076 | 88 633 |
| 100 | 100 | 48 588 | 48 733 | 48 975 | 49 311 | 49 741 |
| 100 | 10 000 | 53 180 | 64 507 | 76 207 | 84 109 | 88 648 |

Table 5. Variation of buckling loads (lb $in^{-1}$) under $N_x$ and $N_y$ for simply–simply case

| | | Initial rotational angles on left side (degrees) | | | | |
|---|---|---|---|---|---|---|
| $\zeta$(lb-in/in$^{-2}$) | $\eta$(lb-in/in$^{-3}$) | case (1) | case (2) | case (3) | case (4) | case (5) |
| 0 | 0 | 24 185 | 24 185 | 24 185 | 24 185 | 24 185 |
| 0 | 10 000 | 26 546 | 32 645 | 40 096 | 46 700 | 51 617 |
| 10 | 100 | 24 221 | 24 294 | 24 416 | 24 586 | 24 803 |
| 10 | 10 000 | 26 557 | 32 653 | 40 102 | 46 703 | 51 619 |
| 100 | 100 | 24 327 | 24 400 | 24 522 | 24 691 | 24 908 |
| 100 | 10 000 | 26 656 | 32 732 | 40 155 | 46 735 | 51 637 |

Table 6. Variation of fundamental natural frequencies (rad $s^{-1}$) for clamped–clamped case

| | | Initial rotational angles on left side (degrees) | | | | |
|---|---|---|---|---|---|---|
| $\zeta$(lb-in/in$^{-2}$) | $\eta$(lb-in/in$^{-3}$) | case (1) | case (2) | case (3) | case (4) | case (5) |
| 0 | 0 | 90.17 | 90.17 | 90.17 | 90.17 | 90.17 |
| 0 | 10 000 | 90.31 | 90.72 | 91.39 | 92.30 | 93.42 |
| 10 | 100 | 90.18 | 90.19 | 90.19 | 90.20 | 90.22 |
| 10 | 10 000 | 90.32 | 90.73 | 91.40 | 92.31 | 93.43 |
| 100 | 100 | 90.27 | 90.27 | 90.28 | 90.29 | 90.30 |
| 100 | 10 000 | 90.41 | 90.81 | 91.48 | 92.39 | 93.50 |

Table 7. Variation of buckling loads (lb $in^{-1}$) under $N_x$ for clamped–clamped case

| | | Initial rotational angles on left side (degrees) | | | | |
|---|---|---|---|---|---|---|
| $\zeta$(lb-in/in$^{-2}$) | $\eta$(lb-in/in$^{-3}$) | case (1) | case (2) | case (3) | case (4) | case (5) |
| 0 | 0 | 102 308 | 102 308 | 102 308 | 102 308 | 102 308 |
| 0 | 10 000 | 102 609 | 103 490 | 104 883 | 106 676 | 108 718 |
| 10 | 100 | 102 332 | 102 341 | 102 356 | 102 377 | 102 404 |
| 10 | 10 000 | 102 630 | 103 510 | 104 901 | 106 692 | 108 732 |
| 100 | 100 | 102 517 | 102 526 | 102 541 | 102 562 | 102 589 |
| 100 | 10 000 | 102 813 | 103 686 | 105 066 | 106 841 | 108 860 |

Table 8. Variation of buckling loads (lb in$^{-1}$) under $N_x$ and $N_y$ for clamped–clamped case

| | | Initial rotational angles on left side (degrees) | | | | |
|---|---|---|---|---|---|---|
| $\zeta$(lb-in/in-$^{2}$) | $\eta$(lb-in/in-$^{3}$) | case (1) | case (2) | case (3) | case (4) | case (5) |
| 0 | 0 | 45 676 | 45 676 | 45 676 | 45 676 | 45 676 |
| 0 | 10 000 | 45 813 | 46 220 | 46 884 | 47 781 | 48 883 |
| 10 | 100 | 45 687 | 45 691 | 45 698 | 45 707 | 45 720 |
| 10 | 10 000 | 45 823 | 46 229 | 46 892 | 47 789 | 48 891 |
| 100 | 100 | 45 770 | 45 774 | 45 781 | 45 790 | 45 803 |
| 100 | 10 000 | 45 905 | 46 311 | 46 971 | 47 865 | 48 962 |

Table 9. Variation of fundamental natural frequencies (rad s$^{-1}$) for free–free case

| | | Initial rotational angles on left side (degrees) | | | | |
|---|---|---|---|---|---|---|
| $\zeta$(lb-in/in-$^{2}$) | $\eta$(lb-in/in-$^{3}$) | case (1) | case (2) | case (3) | case (4) | case (5) |
| 0 | 0 | 29.08 | 29.08 | 29.08 | 29.08 | 29.08 |
| 0 | 10 000 | 29.10 | 29.17 | 29.28 | 29.44 | 29.65 |
| 10 | 100 | 29.12 | 29.12 | 29.12 | 29.12 | 29.13 |
| 10 | 10 000 | 29.14 | 29.21 | 29.33 | 29.49 | 29.69 |
| 100 | 100 | 29.51 | 29.51 | 29.52 | 29.52 | 29.52 |
| 100 | 10 000 | 29.54 | 29.60 | 29.72 | 29.87 | 30.07 |

Table 10. Variation of buckling loads (lb in$^{-1}$) under $N_x$ for free–free case

| | | Initial rotational angles on left side (degrees) | | | | |
|---|---|---|---|---|---|---|
| $\zeta$(lb-in/in-$^{2}$) | $\eta$(lb-in/in-$^{3}$) | case (1) | case (2) | case (3) | case (4) | case (5) |
| 0 | 0 | 10 641 | 10 641 | 10 641 | 10 641 | 10 641 |
| 0 | 10 000 | 10 658 | 10 708 | 10 792 | 10 910 | 11 061 |
| 10 | 100 | 10 673 | 10 674 | 10 674 | 10 676 | 10 677 |
| 10 | 10 000 | 10 690 | 10 740 | 10 824 | 10 942 | 11 092 |
| 100 | 100 | 10 961 | 10 962 | 10 963 | 10 964 | 10 966 |
| 100 | 10 000 | 10 978 | 11 028 | 11 112 | 11 228 | 11 378 |

Table 11. Variation of buckling loads (lb in$^{-1}$) under $N_x$ and $N_y$ for free–free case

| | | Initial rotational angles on left side (degrees) | | | | |
|---|---|---|---|---|---|---|
| $\zeta$(lb-in/in-$^{2}$) | $\eta$(lb-in/in-$^{3}$) | case (1) | case (2) | case (3) | case (4) | case (5) |
| 0 | 0 | 10 393 | 10 393 | 10 393 | 10 393 | 10 393 |
| 0 | 10 000 | 10 409 | 10 460 | 10 543 | 10 660 | 10 809 |
| 10 | 100 | 10 425 | 10 425 | 10 426 | 10 427 | 10 429 |
| 10 | 10 000 | 10 441 | 10 491 | 10 575 | 10 691 | 10 840 |
| 100 | 100 | 10 709 | 10 710 | 10 710 | 10 712 | 10 713 |
| 100 | 10 000 | 10 726 | 10 775 | 10 858 | 10 974 | 11 122 |

Table 12. Variation of fundamental natural frequencies (rad s$^{-1}$) for free–free case (unsymmetric)

| $\zeta_L$ (lb-in/in-$^{2}$) | $\eta_L$ (lb-in/in-$^{3}$) | $W'_{max}$ (left) (degrees) | $\zeta_R$ (lb-in/in-$^{2}$) | $\eta_R$ (lb-in/in-$^{3}$) | $w'_{max}$ (right) (degrees) | $\omega$ (rad s$^{-1}$) |
|---|---|---|---|---|---|---|
| 0 | 10 | $0.100000 \times 10^{-1}$ | 0 | 100 | $0.999987 \times 10^{-2}$ | 29.08 |
| 0 | 10 | $0.100000 \times 10^{-1}$ | 100 | 100 | $0.999868 \times 10^{-2}$ | 29.36 |
| 10 | 10 | $0.100000 \times 10^{-1}$ | 0 | 100 | $0.100079 \times 10^{-1}$ | 29.10 |
| 10 | 10 000 | $0.100000 \times 10^{-1}$ | 100 | 10 000 | $0.986413 \times 10^{-1}$ | 29.94 |
| 100 | 10 | $0.100000 \times 10^{-1}$ | 10 | 10 000 | $0.100788 \times 10^{-1}$ | 29.61 |
| 100 | 10 000 | $0.100000 \times 10^{-1}$ | 100 | 100 | $0.100821 \times 10^{-1}$ | 30.03 |

Table 13. Variation of buckling loads (lb in$^{-1}$) under $N_x$ for free–free case (unsymmetric)

| $\zeta_L$ (lb-in/in-°) | $\eta_L$ (lb-in/in-°$^3$) | $W'_{max}$ (left) (degrees) | $\zeta_R$ (lb-in/in-°) | $\eta_R$ (lb-in/in-°$^3$) | $W'_{max}$ (right) (degrees) | $P_{cr}$ (lb in$^{-1}$) |
|---|---|---|---|---|---|---|
| 0 | 10 | $0.100000 \times 10^{-1}$ | 0 | 100 | $0.999984 \times 10^{-2}$ | 10 643 |
| 0 | 10 | $0.100000 \times 10^{-1}$ | 100 | 100 | $0.999862 \times 10^{-2}$ | 10 755 |
| 10 | 10 | $0.100000 \times 10^{-1}$ | 0 | 100 | $0.100087 \times 10^{-1}$ | 10 654 |
| 10 | 10 000 | $0.100000 \times 10^{-1}$ | 100 | 10 000 | $0.986409 \times 10^{-1}$ | 11 285 |
| 100 | 10 | $0.100000 \times 10^{-1}$ | 10 | 10 000 | $0.100862 \times 10^{-1}$ | 10 993 |
| 100 | 10 000 | $0.100000 \times 10^{-1}$ | 100 | 100 | $0.100898 \times 10^{-1}$ | 11 320 |

Table 14. Variation of buckling loads (lb in$^{-1}$) under $N_x$ and $N_y$ for free–free case (unsymmetric)

| $\zeta_L$ (lb-in/in-°) | $\eta_L$ (lb-in/in-°$^3$) | $W'_{max}$ (left) (degrees) | $\zeta_R$ (lb-in/in-°) | $\eta_R$ (lb-in/in-°$^3$) | $W'_{max}$ (right) (degrees) | $P_{cr}$ (lb in$^{-1}$) |
|---|---|---|---|---|---|---|
| 0 | 10 | $0.100000 \times 10^{-1}$ | 0 | 100 | $0.999982 \times 10^{-2}$ | 10 395 |
| 0 | 10 | $0.100000 \times 10^{-1}$ | 100 | 100 | $0.999842 \times 10^{-2}$ | 10 515 |
| 10 | 10 | $0.100000 \times 10^{-1}$ | 0 | 100 | $0.100086 \times 10^{-1}$ | 10 414 |
| 10 | 10 000 | $0.100000 \times 10^{-1}$ | 100 | 10 000 | $0.986398 \times 10^{-1}$ | 11 079 |
| 100 | 10 | $0.100000 \times 10^{-1}$ | 10 | 10 000 | $0.100873 \times 10^{-1}$ | 10 788 |
| 100 | 10 000 | $0.100000 \times 10^{-1}$ | 100 | 100 | $0.100910 \times 10^{-1}$ | 11 107 |

It should be noted that if both the values of $\zeta$ and $\eta$ are vanished, the plate will be simplified to a simply-supported plate all around, it provides us an exact solution to check. The deviation between the approximate value and analytical result is lower than $+1.3\%$ which is acceptable.

As it can be seen from Table 3, the nonlinear term dominates the fundamental natural frequencies for small values of $\zeta$ and the initial values of rotational angle. For sufficiently large values of $\zeta$ (say, $\zeta/\eta > 1$) the linear term will govern the free vibration behaviour when both values of $\eta$ and $W'$ are large. In Fig. 3, the fundamental frequencies of the plate with elastical restraint for the simply–simply case are plotted against $\eta$. We assume the values of initial rotational angle to be those in case (5), axial forces $N_x$ are identical to be 2000 lb$^{-1}$ in which is less than the critical load. As it can be seen, frequency is nonlinearly increasing with respect to $\eta$. The nonlinearity of frequency is more significant for smaller value of $\zeta$. Table 4 presents the buckling loads of the plate under $N_x$ for different spring constants and different values of initial rotational angle. Table 5 shows the buckling loads when both $N_x$ and $N_y$ applied at the same time. Whenever the values of $\zeta$ and $\eta$ are identical to be zeroes, it also provides an analytical solution to check the approximate solution, and the result is acceptable as before. The characters of the buckling load are very similar to those of the frequency parameters. It can be seen that all values in Table 5 are smaller than those in Table 4 which is reasonable. As it can be seen from Tables 6–8, either free vibration

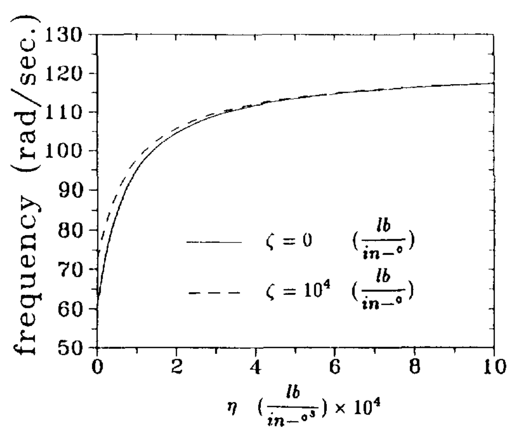


Fig. 3. Fundamental frequency of the plate under axial force $N_x$ for simply–simply case.

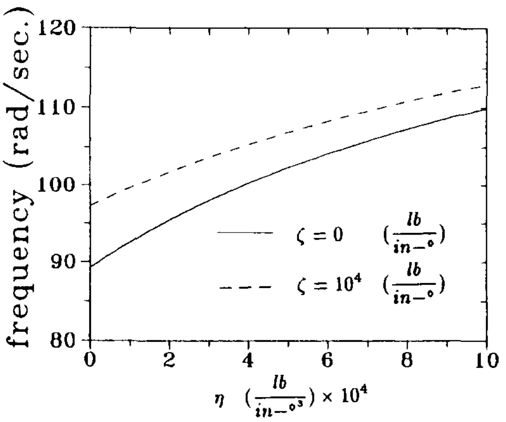


Fig. 4. Fundamental frequency of the plate under axial force $N_x$ for clamped–clamped case.

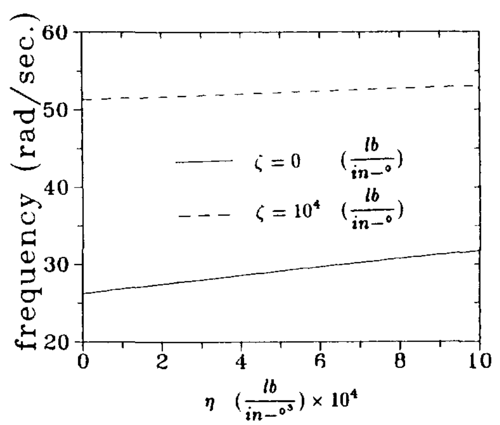


Fig. 5. Fundamental frequency of the plate under axial force $N_x$ for free–free case.

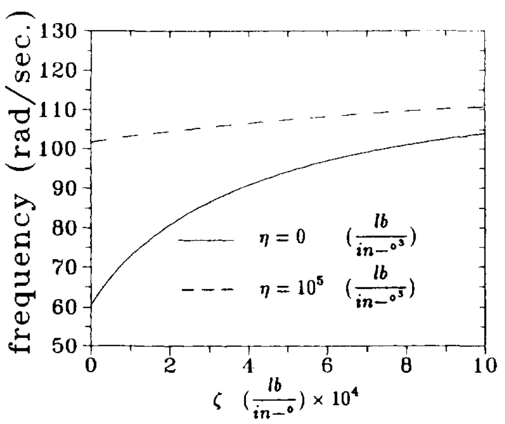


Fig. 6. Fundamental frequency of the plate under axial force $N_x$ for simply–simply case.

behaviour or buckling problem, the characters of the results are similar to those of Tables 3–5. Figure 4 shows the relationship between frequency and $\eta$ is nonlinear if the boundary conditions are assumed to be clamped–clamped. Tables 9–11 and Fig. 5 show that the free vibration and stability behaviours of the plate will not be dominated clearly by the nonlinear restraints, because the stiffness matrix gets smaller when the boundary conditions are released to be the free–free case. Figures 6–8 present the fundamental frequencies of the plate against the linear term $\zeta$ of the restraint, also, the axial forces and initial rotational angles are the same values as those in Figs 3–5. It is evident that the fundamental frequency nonlinearly increases with $\zeta$ even if the boundary condition is the free–free case. All values

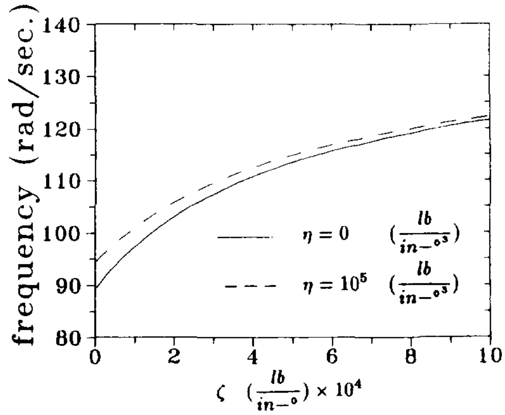


Fig. 7. Fundamental frequency of the plate under axial force $N_x$ for clamped–clamped case.

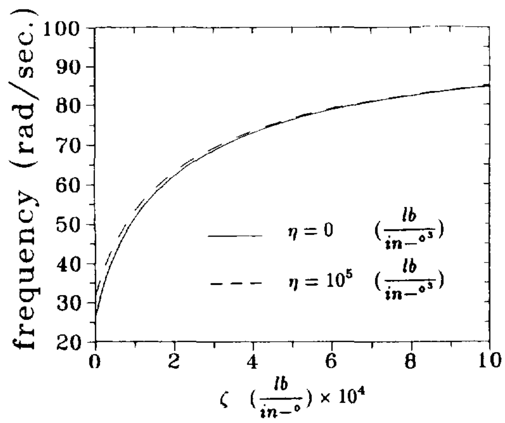


Fig. 8. Fundamental frequency of the plate under axial force $N_x$ for free–free case.

of the free–free plate are smaller than those of the simply–simply and clamped–clamped plate which is expected.

Tables 12–14 present the same analysis except the spring constants are unsymmetric. The columns of $\zeta_L$, $\zeta_R$, $\eta_L$, $\eta_R$ and $W'_L$ are given and the others are evaluated. Noting that we just list the maximum rotational angle of both edges in these tables and the maximum value of $W'_L$ is assumed to be 0.050 for all cases. The iteration scheme is needed which has been stated in the previous section. It can be seen that, the rotational angle values of right edge converge and depend on the spring constants we used. All frequency values and buckling loads in Tables 12–14 are quite reasonable if they are compared with those values of symmetrical cases.

## 4. SUMMARY

The fundamental natural frequencies and buckling loads of a rectangular plate with nonlinearly rotational restraints are obtained by using the finite element technique. The iterative scheme is needed when the rotational springs at both edges are unsymmetric and the results are quite reasonable. The values which describe the free vibration and stability behaviour of the plate will increase when either the parameters of rotational spring or the initial rotational angles increase. Incidentally, it can be concluded that these results grow nonlinearly with respect to either the linear or nonlinear rotational spring constants. Finally, both the frequency and stability parameters are evaluated for several boundary conditions which are quite useful in engineering analysis and design.

## REFERENCES


Bennouna, M. M. and White, R. G. (1984). The effects of large vibration amplitudes on the fundamental mode shape of a clamped–clamped uniform beam. *Journal of Sound and Vibration* **96,** 309–331.

Bhaohyam, G. R. and Prathap, G. (1980). Galerkin finite element method for nonlinear beam vibration. *Journal of Sound and Vibration* **72,** 191–203.

Chi, M., Dennis, Jr, B. G. and Vossoughi, J. (1984). Transverse and torsional vibrations of an axially loaded beam with elastically constrained ends. *Journal of Sound and Vibration* **96,** 235–241.

Den Hartog, J. P. (1936). Forced vibrations in nonlinear systems with various combinations of linear springs. *Journal of Applied Mechanics* **3,** A127–A130.

Dokainish, M. A. and Kumar, R. (1971). Experimental and theoretical analysis of the transverse vibrations of a beam having bilinear support. *Experimental Mechanics, Journal of SESA.* **11**(6), 263–270.

Evensen, D. A. (1968). Nonlinear vibrations of beams with various boundary conditions. *American Institute of Aeronautics and Astronautics Journal* **6,** 370–372.

Gutierrez, R. H., Laura, P. A. A. and Rossi, R. E. (1990). Natural frequencies of a Timoshenko beam of non-uniform cross-section elastically restrained at one end and guided at the other. *Journal of Sound and Vibration* **141,** 174–179.

Gutierrez, R. H., Laura, P. A. A. and Rossi, R. E. (1991). Fundamental frequency of vibration of a Timoshenko beam of non-uniform thickness. *Journal of Sound and Vibration* **145,** 341–344.

Laura, P. A. A. and Romanelli, E. (1974). Vibrations of rectangular plates elastically restrained against rotation along all edges and subject to a biaxial state of stress. *Journal of Sound and Vibration* **37,** 367–377.

Lee, S. Y. and Ke, H. Y. (1990). Free vibrations of a non-uniform beam with general elastically restrained boundary conditions. *Journal of Sound and Vibration* **136,** 425–437.

Liu, W. H., Kou, H. S. and Yang, F. S. (1988). Nonlinear vibrations of beams with elastically restrained edges. *Journal of Sound and Vibration* **121,** 375–381.

Maurizi, M. J. and Belles, P. M. (1991). General equation of frequencies for vibrating uniform one-span beams under compressive axial loads. *Journal of Sound and Vibration* **145,** 345–347.

Maurizi, M. J., Rossi, R. E. and Belles, P. M. (1990). Free vibration of uniform Timoshenko beam with ends elastically restrained against rotation and translation. *Journal of Sound and Vibration* **141,** 359–362.

Paslay, P. R. and Gurtin, M. E. (1960). The vibration response of a linear undamped systems resting on a nonlinear spring. *Journal of Applied Mechanics, Transactions of the ASME* **27,** 272–274.

Picard, A., Beaulieu, D. and Perusse, B. (1987). Rotational restraint of a simple column base connection. *Canadian Journal of Civil Engineering* **14,** 49–57.

Porter, B. and Billet, R. A. (1965). Harmonic and sub-harmonic vibration of a continuous system having nonlinear constraint. *International Journal of Mechanical Science* 7(6), 431–439.

Prathap, G. (1978). Nonlinear vibration of beams with variable axial restraint. *American Institute of Aeronautics and Astronautics Journal* **16,** 622–624.

Sarma, B. S. and Varadan, T. K. (1983). Lagrange-type formulation for finite element analysis of nonlinear beam vibration. *Journal of Sound and Vibration* **86,** 61–70.

Srinivasan, A. V. (1965). Large amplitude free oscillations of beams and plates. *American Institute of Aeronautics and Astronautics Journal* **3,** 1151–1153.

Taucher, T. R. and Ayre, R. S. (1965). Shock response of a simple beam on nonlinear supports. *Journal of Engineering Mechanics Division, Proceedings of the ASCE* 91–109.

Timoshenko, S. P. and Gere, J. M. (1961). *Theory of Elastic Stability*, 2nd edn. McGraw-Hill, New York.

Venkateswara Rao, G. and Rajasekhara Naidu, N. (1994). Free vibration and stability behaviour of uniform beams and columns with nonlinear elastic end rotational restraints. *Journal of Sound and Vibration* **176,** 130–135.

Wah, T. (1964). The normal modes of vibration of certain non-linear continuous systems. *Journal of Applied Mechanics* **7,** 139–140.

Warburton, G. B. and Edney, S. L. (1984). Vibrations of rectangular plates with elastically restrained edges. *Journal of Sound and Vibration* **95,** 537–552.

Woinowsky-Krieger, S. (1950). The effect of an axial force on the vibration of hinged bars. *Journal of Applied Mechanics* **17,** 35–36.